

Short Communication

## Vacancy Assisted Li Intercalation in Crystalline Si as Anode Materials for Lithium Ion Batteries

Jinmei Huang<sup>1</sup>, Zhiqiang Wang<sup>1</sup>, Xin Gong<sup>1</sup>, Musheng Wu<sup>1</sup>, Gang Liu<sup>1</sup>, Xueling Lei<sup>1</sup>, Jianxiong Liang<sup>2</sup>, Hanbiao Cao<sup>2</sup>, Fenjin Tang<sup>2</sup>, Minsheng Lei<sup>1</sup>, Bo Xu<sup>1,3</sup>, Chuying Ouyang<sup>1,3,\*</sup>

<sup>1</sup> Department of Physics, Jiangxi Normal University, Nanchang, 330022, P. R. China

<sup>2</sup> Jiangxi ZT New Energy Co. Ltd, Guangfeng, 334600, China

<sup>3</sup> Key Laboratory for Advanced Functional materials of Jiangxi Province, Nanchang, 330022, P. R. China

\*E-mail: [cyouyang@jxnu.edu.cn](mailto:cyouyang@jxnu.edu.cn)

Received: 17 February 2013 / Accepted: 19 March 2013 / Published: 1 April 2013

---

Silicon is one important candidate as anode materials for next generation lithium ion batteries because of its extremely high specific capacity (4200mAh/g). In this paper, we show from first principles calculations that vacancies play important role in the beginning of the lithiation process of crystalline silicon. Without vacancy, the Li binding energy is lower than that of Li metal, indicating that lithium can not be intercalated into crystalline Si. On the other hand, vacancies can enhance the binding energy substantially and make the lithium intercalation process thermodynamically favorable during the initial stage of the discharge process.

---

**Keywords:** Lithium ion batteries; Silicon anode; Vacancy; Binding energy

### 1. INTRODUCTION

Lithium ion batteries have attracted more and more attention in both the academic and industrial fields [1]. Over the past three decades, numerous studies aimed at the improvement of the specific capacity of the electrode materials for lithium ion batteries. Silicon is of significant interest as an alternative to graphite anode material due to its extremely high theoretical capacity (4200 mAh/g) [2-4]. However, the Si anode material undergoes very large volume expansion upon lithium intercalation and therefore suffers from poor cycling performance [5]. Using *in situ* X-ray diffraction techniques, Obrovac et al. [6] showed that crystalline silicon is converted to amorphous Si during the lithiation process, in which structural transition occurs from crystalline phase to amorphous  $\text{Li}_x\text{Si}$  phases gradually.

Although there are many papers studied the lithium intercalation process of Si anode materials, little is known about the dynamic processes at the atomic level. To have fundamental insights into these issues, density functional theory (DFT) electronic structure calculations and molecular dynamics simulations may provide essential information from the atomic level. Tritsarlis et al. [7] studied the lithium ion diffusion in bulk and amorphous silicon from first principles calculations. A double- $\zeta$  plus polarization basis set was used and they observed that lithium migration in crystalline silicon between tetrahedral interstitial sites has an energy barrier of 0.55 eV. Chevrier et al. [8] has studied the basic physical and chemical characteristics of  $\text{Li}_x\text{Si}$  alloy phases from density functional theory. They also created a protocol to simulate the lithiation of amorphous Si at room temperature in conjunction with results from first principles calculations [9]. More recently, Chan et al. [10] studied the electrochemical lithiation and delithiation of faceted crystalline silicon from *ab initio* molecular dynamics simulations using slab models, and gave a good explanation to the anisotropy of the lithiation observed in experiments.

As for lithium intercalation in bulk silicon, Wan et al. have studied dilute lithium intercalated in crystalline Si [11]. They observed single Li prefers to stay at the  $T_d$  sites with a binding energy of 1.359 eV, which is smaller than the binding energy of lithium metal ( $\sim 1.8$  eV) [12]. This indicates that lithium can not be intercalated into the crystalline Si lattice upon discharging of the Si-Li metal half battery to even 0 V. They have also studied the lithium insertion process into the silicon nanowires (SiNWs) [13]. They found that the [110] SiNWs with different diameters always present the highest binding energies on various insertion locations. However, even the highest binding energies they obtained from their calculation are slightly smaller than that of lithium metal.

In the present work, we show from first principles calculations that the interaction between Si atom and dilute Li atoms in crystalline silicon is very weak. Although  $T_d$  interstitial sites in Si lattice provide space for lithium storage, the electronic interaction between them is weak. Then, we show that vacancies will enhance the interaction and thus the binding energy of dilute Li atom in defective silicon will be higher than that of in lithium metal, which ensures the intercalation of Li into the silicon crystalline thermodynamically favorable.

## 2. COMPUTATIONAL DETAILS

Calculations in this work are performed within the density-functional theory (DFT) and the plane-wave pseudopotential method, which are implemented in the Vienna *ab initio* simulation package (VASP) [14, 15]. The core ion and valence electron interaction are described by the projector augmented wave method (PAW) [16] and the exchange-correlation part is described with the generalized gradient approximation (GGA) by Perdew and Wang (PW91) [17]. The Monkhorst-Pack [18] scheme  $k$ -point sampling with  $7 \times 7 \times 7$  (for unitcell cases) and  $3 \times 3 \times 3$  (for  $2 \times 2 \times 2$  supercell) grids has been used for the integration of the Brillouin zone. Energy cut off for the plane waves is chosen to be 500 eV. The lattice parameters and the atomic position are fully relaxed, and the final forces on all relaxed atoms are less than  $0.005 \text{ eV}\text{\AA}^{-1}$ .

### 3. RESULTS AND DISCUSSION

Silicon is iso-structural with the diamond. The optimized lattice constant is 5.46 Å, which is a little bit over estimated comparing to the experimental value 5.43 Å [19]. As we know, only half of the tetrahedral sites ( $T_d$  sites) are occupied by Si atoms in the unitcell and the other half are empty. Therefore, when lithium atoms are intercalated into the silicon unit cell, they will first take those empty  $T_d$  sites, as shown in Fig. 1.

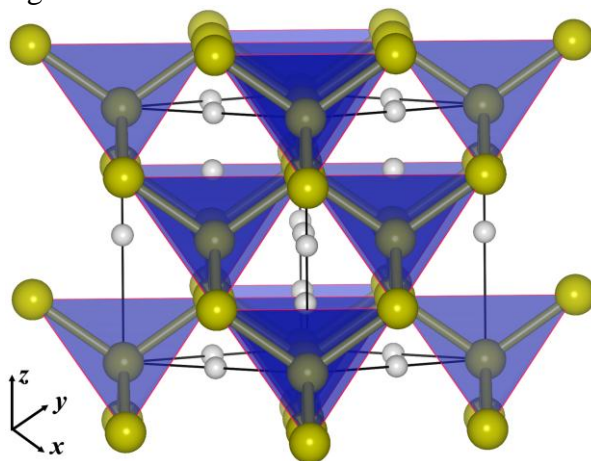


**Figure 1.** Schematic views of crystalline structure of silicon in the ball and stick mode. The large (yellow) spheres are Si atoms, while the small (white) spheres indicate the empty tetrahedral sites in the silicon unit cell. “x” , “y” and “z” refer to the orientation of the lattice vectors.

In our simulation, we first put one Li atom in the center of the unitcell, which is one of the 8 empty  $T_d$  sites. We denote the system as  $Si_8Li_1$ . After relaxation of the atomic positions and the lattice constant, we observed that the volume of the unitcell is expanded and the lattice constant increases from 5.46 Å to 5.52 Å, corresponding to a 2.9 % volume expansion. The Li atom in the  $T_d$  site pushes its neighboring Si atoms away from the  $T_d$  site center, and the Li-Si distance increases from 2.364 Å to 2.454 Å. As a result, the  $Si_4$  tetrahedral is distorted and the four Si-Si bonds are no longer equivalent. One bond becomes shorter (2.327 Å) while the other three become longer (2.412 Å), comparing to the equilibrium Si-Si bond length of 2.364 Å. This distortion substantially decreases the binding energy of the lithium intercalated silicon, which makes it energetically unfavorable for the lithium intercalation into the silicon lattice. The calculated binding energy is about 1.37 eV, in agreement with results from Ref. [11]. To describe this situation with an electrochemical parameter, we calculated the average lithium intercalation potential defined as:  $V_{ave} = -\Delta E/nF$ , where  $F$  is the Faraday constant,  $n$  is the number of lithium ions intercalated in the lattice, and  $\Delta E = E_{tot}[Si_8Li] - E_{tot}[Si_8] - E_{tot}[Li_{bcc}]$ , is the total energy difference defined with metallic Li as reference [20, 21]. The calculated intercalation potential is -0.51 V, indicating that lithium can not be intercalated into silicon material even when the material is discharged to 0 V. The negative intercalation potential indicates that the free energy of the system is lower when lithium is in the form of metallic Li, which results in the formation of Li metal at the Si electrode surface [22]. When more lithium are intercalated into the lattice, the binding energy

becomes higher and when all the empty  $T_d$  sites are taken by lithium atoms ( $Li_8Si_8$ ), the average intercalation potential becomes -0.14 V.

The band structures of the  $Si_8$  and  $Si_8Li_1$  are given in Fig. 2, from which we can see that the Fermi level is shifted to the conduction band and the states around the  $\Gamma$ -point becomes occupied, indication of the metallic characteristic of the lithiated system. Furthermore, the shape and dispersion of the energy bands are not changed when the lithium atom is intercalated into the lattice, while the degeneracy is decreased and each band is split into two or more bands. This shows that the interaction between the Si host matrix and the intercalated lithium atom is not strong. On the other hand, as the Si-Si bond lengths near the Li atom is changed due to the electrostatic potential of Li atom, which decreases the Si-Si bond strength and thus increases the total energy of the system. As a result, Li is not ready to insert into the Si lattice and hence we observed the negative intercalation voltage.

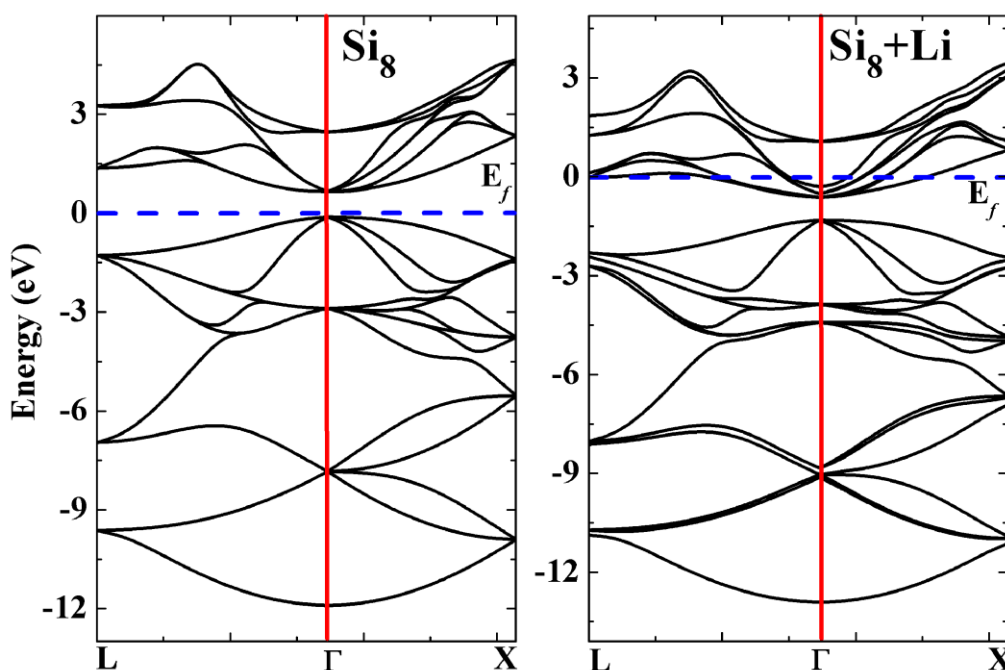


**Figure 2.** The band structures of the Si unitcell ( $Si_8$ , left) and the Si unitcell with one Li in the center ( $Si_8Li_1$ , right).

The weak interaction between Si and Li in  $Si_8Li_1$  can be confirmed through analyzing the charge density of the systems. Bader charge analysis shows that each Li atom loses 0.82e charge and becomes positively charged. Fig. 3 gives the charge density contour of crystalline silicon ( $Si_8$ ), crystalline silicon with Li occupied all the  $T_d$  sites ( $Si_8Li_8$ ), and  $Si_1Li_1$  alloy phase that was observed experimentally [23]. As it can be seen, strong Si-Si covalent bonds are formed in crystalline silicon since the majority of the charge is distributed in the middle of every two Si atoms (see Fig. 3a). On the other hand, the charge is localized around Si atoms in Fig. 3b, indicating the bonding effect between Si atoms is weakened. In the case of the  $Si_1Li_1$  alloy, we also observed that some portion of the charge distributes in the middle of two Si atoms, but not as much as crystalline Si (see Fig. 3c). This indicates

that the strength of the Si-Si covalent bond in  $\text{Si}_1\text{Li}_1$  alloy is stronger than lithiated silicon while weaker than crystalline silicon. As a result, the binding energy of  $\text{Si}_1\text{Li}_1$  alloy is much larger than the lithiated crystalline silicon. We also calculated the average intercalation potential for  $\text{Si}_1\text{Li}_1$  alloy and we obtained 0.42 V, in contrast to the -0.14 V for lithiated crystalline silicon  $\text{Li}_8\text{Si}_8$ .

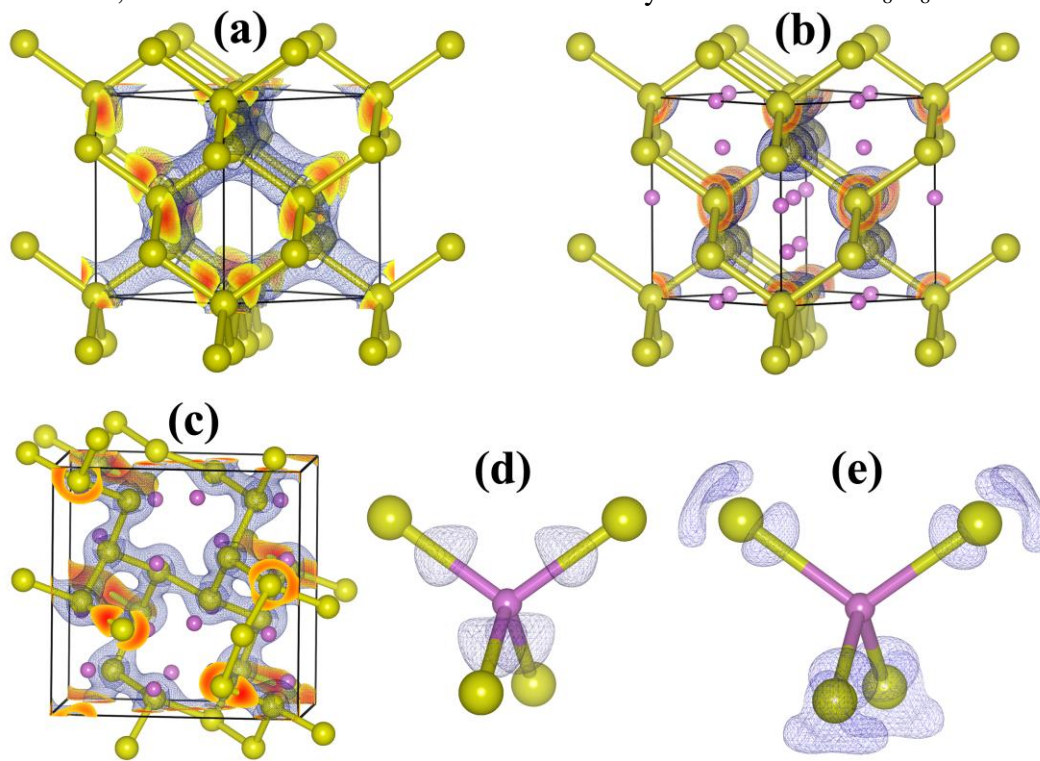


**Figure 3.** Charge density contours for crystalline silicon (a), lithiated crystalline silicon  $\text{Li}_8\text{Si}_8$  (b), and  $\text{Li}_1\text{Si}_1$  alloy (c), and differential charge density contours for  $\text{Si}_8$  (d) and  $\text{Si}_7\text{Vac}_1$  (e). The large (yellow) and the small (purples) spheres are Si and Li atoms, respectively. The charge density isosurface values are  $0.42 \text{ e}/\text{\AA}^3$  for cases (a) to (c) and  $0.02 \text{ e}/\text{\AA}^3$  for cases (d) and (e), respectively.

From the above discussion, we can see that lithium intercalate into crystalline silicon is energetically unfavorable, while it is energetically favorable to form  $\text{Li}_x\text{Si}_1$  alloy. In fact, silicon as lithium storage material is exactly due to the formation of various  $\text{Li}_x\text{Si}$  alloys. Then, another problem arises: how does lithium intercalated into the silicon lattice before  $\text{Li}_x\text{Si}$  alloy phases are formed when silicon is applied as anode and operates under room temperature. Here we show that vacancies play important role to assist lithium intercalation into crystalline silicon before the  $\text{Li}_x\text{Si}_y$  alloy phases formed.

In order to simulate the vacancy assisted lithium intercalation process, we used a  $2 \times 2 \times 2$  supercell containing 63 Si atoms and one vacancy in the center of the supercell ( $\text{Si}_{63}\text{Vac}_1$ ). We put one lithium atom in the  $2 \times 2 \times 2$  lattice, and we find that the binding energy becomes higher than Li metal (and thus positive intercalation potential). Furthermore, we notice that the vacancy has a trapping effect to the lithium atom. The binding energy is 2.62 eV when the lithium stays at the vacancy center and gradually becomes smaller when the lithium moves away from the vacancy. Fig. 4 shows the binding energies as a function of the Li-vacancy distance. It shows clearly that when the Li-vacancy

distance is larger than 4 Å, the trapping effect is disappeared and the binding energy is approximately 2.08 eV. Obviously, the lithium binding energy in the defective silicon is enhanced and become higher than that of lithium metal [12], and the average intercalation potential for lithium insertion into defective silicon becomes positive.

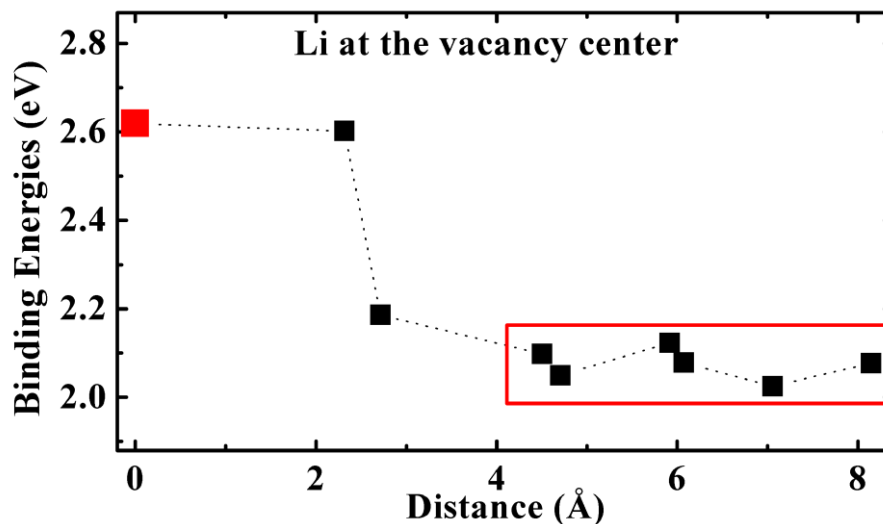


**Figure 4.** Binding energies of the lithium atom intercalated in the  $\text{Si}_{63}\text{Vac}_1$  lattice. The horizontal axis is the distance between the lithium atom and the vacancy center.

The physics behind the vacancy enhanced binding energy can also be shown from the charge density analysis. Fig. 3d and 3e present the charge density difference between the lithiated silicon and pure silicon. The charge density difference is defined as  $\rho_{\text{diff}} = \rho[\text{Si}+\text{Li}] - \rho[\text{Si}]$ , where  $\rho[\text{Si}+\text{Li}]$  and  $\rho[\text{Si}]$  are the charge density of lithiated silicon and pure silicon, respectively. With this definition, integration of the charge density difference over the unit cell will obtain one electron, as there is one more electron in the lithiated silicon unit cell than the pure silicon unit cell. Fig. 3d and 3e are for cases of perfect silicon ( $\text{Si}_{64}$ ) and defective silicon ( $\text{Si}_{63}\text{Vac}_1$ ), respectively. We can see that in both cases, the Li atom is fully ionized. For pure silicon, the charge from ionization of the Li atom distributes around the lithium atom, which does not form bonds with silicon atoms. On the other hand, for the case of the defective silicon, the charge transfers from the Li atom to the nearby Si atoms. The vacancy creates dangling bonds to its nearest neighboring Si atoms. These Si atoms have unpaired electrons and the charge transferring from Li to the Si atoms will partly saturate those unpaired electrons, which lower the energy of the system.

#### 4. SUMMARY AND CONCLUSIONS

In summary, our first principles calculation results predict that vacancies are important in the initial stage of the lithiation process of crystalline silicon as anode materials for lithium ion batteries. Vacancies in silicon are in favor of the lithium binding with the silicon matrix, the binding energy is substantially enhanced by the vacancy and the average potential increases from -0.51 eV for single Li atom intercalation into  $T_d$  sites in perfect silicon lattice to 0.20 eV for that of mono-vacancy defective

silicon. The physics behind the vacancy enhanced binding energy is related with the distribution of the excess electron from ionization of the lithium atom, which is fully ionized in the silicon crystal. Vacancy creates dangling bonds to its neighboring Si atoms and the excess charge will saturate the unpaired electron of the dangling bonds. As a result, the binding energy increases from 1.37 eV to 2.08 eV, which makes the electrochemical intercalation of lithium into the crystalline silicon possible from the thermodynamics point of view.

#### ACKNOWLEDGEMENT

Thanks to the support of NSFC under Grant Nos. 11064004, 11234013 and 11264014. C. Y. Ouyang is also supported by the “Gan-po talent 555” Project of Jiangxi Province and the oversea returned project from the Ministry of Education. B. Xu is supported by the Sponsored Program for Cultivating Youths of Outstanding Ability in Jiangxi Normal University. Computations are performed at Tianjing High Performance Computer Center.

#### References

1. J. M. Tarascon, and M. Armand, *Nature* 414 (2001) 359.
2. X. H. Liu, J. W. Wang, S. Huang, F. F. Fan, X. Huang, Y. Liu, S. Krylyuk, J. Yoo, S. A. Dayeh, A. V. Davydov, S. X. Mao, S. T. Picraux, S. L. Zhang, J. Li, T. Zhu, and J. Y. Huang, *Nature Nanotechnology* 7 (2012) 749.
3. S. Misra, N. Liu, J. Nelson, S. S. Hong, Y. Cui, and M. F. Toney, *ACS Nano* 6 (2012) 5465.
4. K. Kang, H. S. Lee, D. W. Han, G. S. Kim, D. H. Lee, G. Lee, Y. M. Kang, and M. H. Jo, *Appl. Phys. Lett.* 96 (2010) 053110.
5. U. Kasavajjula, C. Wang, A. J. Appleby, *J. Power Sources* 163 (2007) 1003.
6. M. N. Obrovac and L. Christensen, *Electrochem. Solid-State Lett.* 7 (2004) A93.
7. G. A. Tritsarlis, K. J. Zhao, O. U. Okeke, and E. Kaxiras, *J. Phys. Chem. C* 116 (2012) 22212.
8. V. L. Chevrier, J. W. Zwanziger, and J. R. Dahn, *Can. J. Phys.* 87 (2009) 625.
9. V. L. Chevrier, J. R. Dahn, *J. Electrochem. Soc.* 156 (2009) A454.
10. M. K. Y. Chan, C. Wolverton, J. P. Greeley, *J. Am. Chem. Soc.* 134 (2012) 14362.
11. W. H. Wan, Q. F. Zhang, Y. Cui, and E. G. Wang, *J. Phys.: Condens. Matter.* 22 (2010) 415501.
12. K. Doll, N. M. Harrison, and V. R. Saunders, *J. Phys.: Condens. Matter.* 11 (1999) 5007.
13. Q. F. Zhang, W. X. Zhang, W. H. Wan, Y. Cui, and E. G. Wang, *Nano Lett.* 10 (2010) 3243.
14. G. Kresse, J. Hafner, *Phys. Rev. B* 48 (1993) 13115.
15. G. Kresse, J. Furthmuller, *Phys. Rev. B* 54 (1996) 11169.
16. P. E. Blochl, *Phys. Rev. B* 50 (1994) 17953.
17. Y. Wang, J. P. Perdew, *Phys. Rev. B* 44 (1991) 13298.
18. H. J. Monkhorst, J. D. Pack, *Phys. Rev. B* 13 (1976) 5188.
19. D. M. Toebbens, N. Stuesser, K. Knorr, H. M. Mayer, and G. Lampert, *J. Appl. Phys.* 45 (1974) 1456.
20. C. Y. Ouyang, Z. Y. Zhong, M. S. Lei, *Electrochem. Commun.* 9 (2007) 1107.
21. C. Wolverton, A. Zunger, *Phys. Rev. B* 57 (1998) 2242.
22. Z. Y. Zhong, C. Y. Ouyang, S. Q. Shi, and M. S. Lei, *ChemPhysChem* 9 (2008) 2104.
23. L.A. Stearns, J. Gryko, J. Diefenbacher, G. K. Ramachandran, and P. F. McMillan, *J. Solid State Chem.* 173 (2003) 251.